DRAFT VERSION MAY 7, 2020
Typeset using LaTeX **twocolumn** style in AASTeX62

Cluster Difference Imaging Photometric Survey (CDIPS) II: A Jupiter-Sized Planet in IC 2602

L. G. BOUMA,[1] R. BRAHM,[2,3,4] J. D. HARTMAN,[1] P. EVANS,[5] G. ZHOU,[6] J. DE LEON,[7] K. G. STASSUN,[8,9] K. A. COLLINS,[6] S. N. QUINN,[6] C. ZIEGLER,[10] J. LIVINGSTON,[7] T. HENNING,[11] A. JORDÁN,[12,4] N. ESPINOZA,[13] W. BHATTI,[1] J. N. WINN,[1] G. Á. BAKOS,[1] G. R. RICKER,[14] R. VANDERSPEK,[14] D. W. LATHAM,[6] S. SEAGER,[15] J. M. JENKINS,[16] AND TSO/SPOC/POC REPRESENTATIVES

[1]*Department of Astrophysical Sciences, Princeton University, 4 Ivy Lane, Princeton, NJ 08540, USA*
[2]*Center of Astro-Engineering UC, Pontificia Universidad Católica de Chile, Av. Vicuña Mackenna 4860, 782-0436 Macul, Santiago, Chile*
[3]*Instituto de Astrofísica, Facultad de Física, Pontificia Universidad Católica de Chile, Av. Vicuña Mackenna 4860, 782-0436 Macul, Santiago, Chile*
[4]*Millennium Institute of Astrophysics, Av. Vicuña Mackenna 4860, 782-0436 Macul, Santiago, Chile*
[5]*El Sauce Observatory, Coquimbo Province, Chile*
[6]*Center for Astrophysics | Harvard & Smithsonian, 60 Garden St, Cambridge, MA 02138, USA*
[7]*Department of Astronomy, University of Tokyo, 7-3-1 Hongo, Bunkyo-ky, Tokyo 113-0033, Japan*
[8]*Vanderbilt University, Department of Physics & Astronomy, 6301 Stevenson Center Lane, Nashville, TN 37235, USA*
[9]*Fisk University, Department of Physics, 1000 17th Avenue N., Nashville, TN 37208, USA*
[10]*Dunlap Institute for Astronomy and Astrophysics, University of Toronto, 50 St. George Street, Toronto, Ontario M5S 3H4, Canada*
[11]*Max-Planck-Institut für Astronomie, Königstuhl 17, 69117 Heidelberg, Germany*
[12]*Facultad de Ingeniería y Ciencias, Universidad Adolfo Ibáñez, Av. Diagonal las Torres 2640, Peñalolén, Santiago, Chile*
[13]*Space Telescope Science Institute, 3700 San Martin Drive, Baltimore, MD 21218, USA*
[14]*Department of Physics and Kavli Institute for Astrophysics and Space Research, Massachusetts Institute of Technology, Cambridge, MA 02139, USA*
[15]*Department of Earth, Atmospheric, and Planetary Sciences, Massachusetts Institute of Technology, Cambridge, MA 02139, USA*
[16]*NASA Ames Research Center, Moffett Field, CA 94035, USA*

(Received May 7, 2020; Revised —; Accepted —)

Submitted to AAS journals.

ABSTRACT

We report the discovery of the transiting planet TOI 837.01, a warm Jupiter-sized planet (R_p = 10.*XX* $R_\oplus$, P = 8.*YY* d), with mass less than X.XX M_{Jup}. TOI 837.01 orbits a V=10.6, T=9.9 G-dwarf in IC 2602, also known as the "Southern Pleiades", and is therefore 50 million years old. We characterize the system using data from the NASA *Transiting Exoplanet Survey Satellite* (TESS), the ESA Gaia mission, ground-based photometry, and spectroscopy from CTIO1.5/CHIRON, XXX/FEROS, and AAT/Veloce. TOI 837.01 joins the growing ranks of adolescent exoplanets orbiting bright host stars, and is amenable for studies of planetary atmospheric and orbital evolution.

Keywords: Exoplanets (XXX), Exoplanet evolution (491), Stellar ages (1581), Young star clusters (XXX)

1. INTRODUCTION

Recently, young planets have been hype.
Section 2 Section 3 Section 4 Section 5 Section 6.

2. THE DATA

2.1. *TESS Photometry*

TOI 837 (TIC 460205581, GAIA DR2 5251470948229949568) was observed by the TESS spacecraft from X to Y in two-minute cadence mode.
Figure 1.

Corresponding author: L. G. Bouma
luke@astro.princeton.edu

2.2. *Ground-based Time-Series Photometry*

2.3. *Imaging*

2.4. *Spectroscopy*

2.4.1. *CHIRON*

9 spectra with CTIO1.5/CHIRON, from January 28 through March 14, 2020. 6 were usable.

2.4.2. *FEROS*

N spectra with XXX/FEROS

2.4.3. *Veloce*

M spectra with AAT/Veloce.

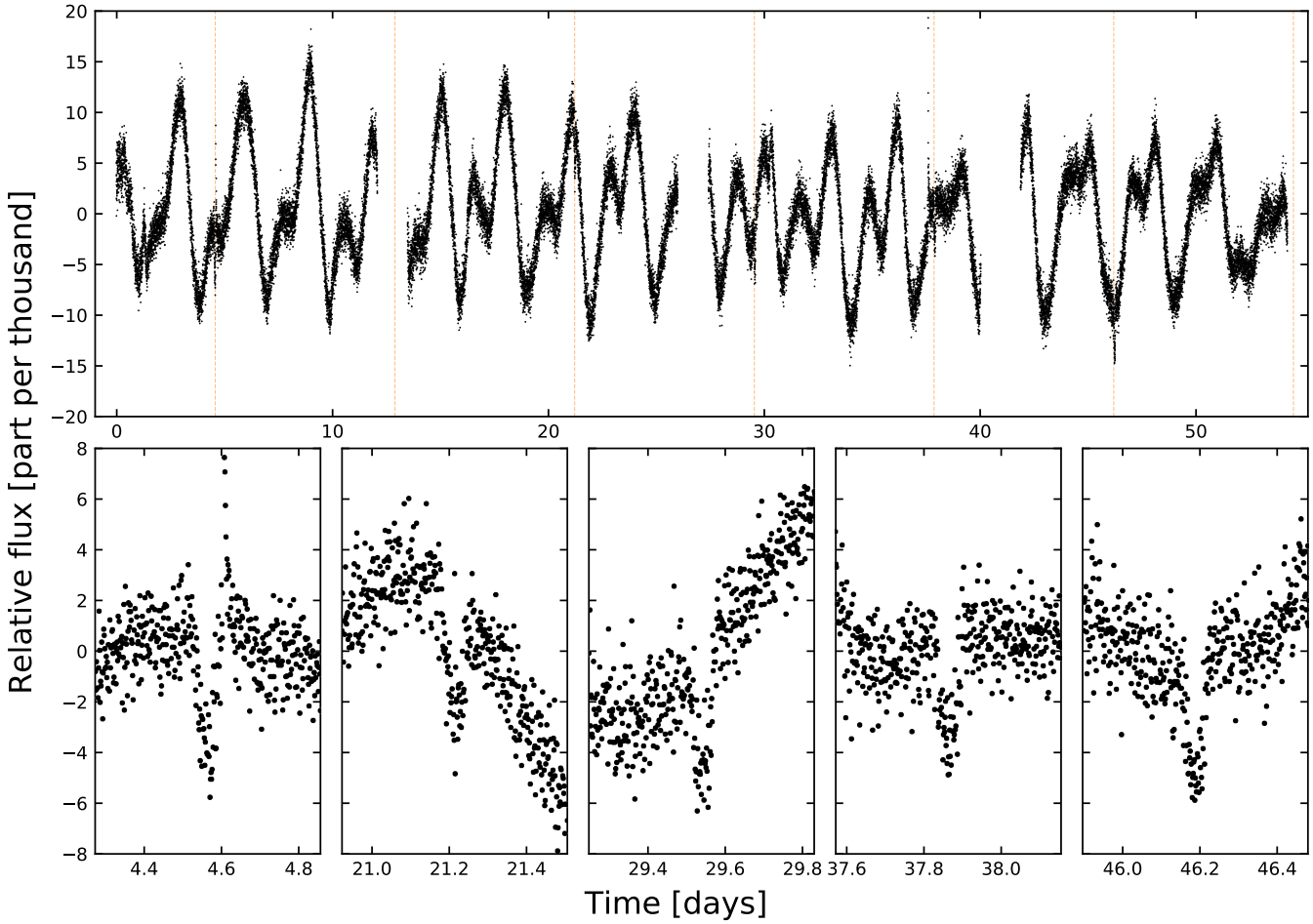

Figure 1. TESS lightcurve of TOI 837 (Sectors 10 and 11). *Top*: PDCSAP mean-subtracted relative flux at 2-minute sampling. Spot-induced stellar variability is the dominant signal. Dashed lines show the five transits observed by TESS. *Bottom*: Zoomed windows of individual transits.

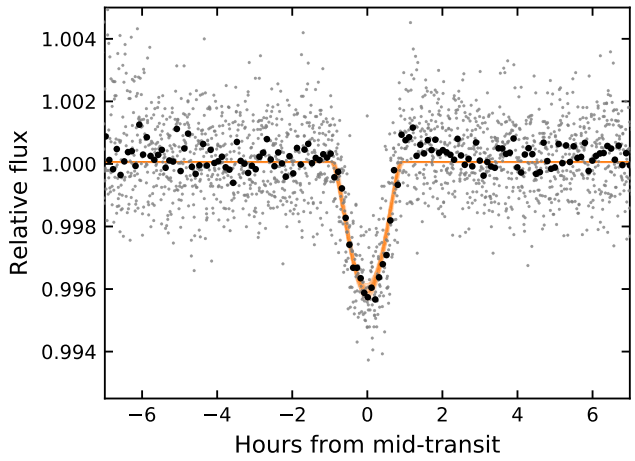

Figure 2. Phase-folded transit of TOI 837.01. Gray points are 2-minute PDCSAP flux measurements, detrended with a 0.3-day robust Huber spline (see Section 2.1). Black points are binned to approximately 1 point per 6 minutes. One hundred samples from the posterior are shown with orange lines.

2.5. *Astrometry*

3. THE STAR

3.1. *The Cluster*

IC 2602 canonically has an age of 30 ± 20 Myr (CITE: Van Leeuwen 2009). Or logage between 7.533 and 7.563 (Bossini et al. 2019).

Or Li age of 40-50Myr (David+19, comparison with other Li stars).

Reported mean metallicity values [Fe/H] for the cluster range between slightly super-solar (0.04 ± 0.01, Baratella et al. 2020) and slightly sub-solar (-0.02 ± 0.02, Netopil et al. 2016).

IC 2602 is supervirial, in the sense that the observed stellar velocity dispersion is larger than the value expected if it were in virial equilibrium by about a factor of two (Bravi et al. 2018).

3.2. *Cluster Membership*

The Gaia kinematics are good; gamma velocity is correct; Li (FEROS + Veloce) is strong; the rotation period and vsini agree with sub-Pleiades age expected for an IC 2602 member.

3.2.1. *Kinematics*

Gaia

3.2.2. *Rotation*

TESS photometric rotation period = 3.5days ish.
vsini = 17.48 ± 0.15 (CHIRON).
The two agree.
For comparison, gyrochrones would predict X.XX.
This implies sub-Pleiades age expected for an IC 2602 member.

3.2.3. *Lithium*

Rafael's co-added FEROS spectra gave a Li doublet equivalent width of 154 milliangstrom (see attached).

As a reminder, Teff=6100K (TICv8). Or Teff = 5946 ± 39 (CHIRON). Rafael, if you have a better determination of Teff, it would be helpful! SpType is early-G, late-F from your quicklook spectral typing earlier.

Relevant colors are V-K = 1.7, V-I = V-T = 0.7

Summarizing relevant lithium facts:

Lithium depletion for a star of TOI-837's spectral type happens over timescales >100 Myr (Soderblom+2013). This is because the convective envelopes are very shallow, so they don't cycle material down to the >3e6 K core until much later.

Nonetheless, comparison of early-G field stars to e.g., 600 Myr old Hyads shows that the depletion does happen over gigayear timescales (Berger+2018, fig 7).

Comparing to the Li EWs measured by Berger+2018 (their Fig 5), TOI-837 is consistent with being younger than almost all CKS planet-hosting field stars.

The TOI-837 Li EW measured here (150 milliangstrom) is consistent with what's seen for stars of similar colors in <100 Myr old moving groups (Elliott+2016, Fig 11 – attached). This is sensible, because IC 2602 is supposed to be 50 Myr old.

3.2.4. *Literature Membership*

The membership of TOI 837 in IC 2602 was noted by Oh et al. (2017), in what they dubbed "Group 5". Analyzing the clusters of Oh et al. (2017), **?** fitted the Gaia, 2MASS, and WISE photometry with MIST isochrones, and reported stellar masses, radii, metallicities, ages, distances, and extinction for 9754 stars, including TOI 837.

TOI 837 was also listed as a member of "Theia 92" by **?**. These authors identified 999 candidate cluster members, and reported a cluster isochrone age $\log t = 7.55$ with uncertainty ≈ 0.15 dex.

3.3. *Stellar Parameters*

3.3.1. *Physical*

(Lstar, Rstar, Teff, Age and Mstar)
Figure 3.

Astrometric information—The RUWE (CITE, CITE) for TOI 837 is 1.02, indicative that there are no obviously present astometric companions.

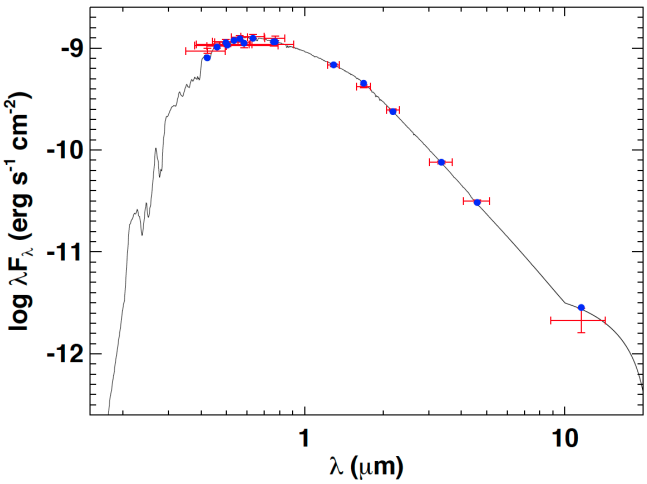

Figure 3. Spectral energy distribution of TOI 837 from archival photometry. Keivan: please describe!

3.3.2. *Rotation*

Stellar vsini Stellar rotation

3.4. *RVs*

I don't strongly expect the Veloce RVs or the FEROS ones to lead to a mass measurement. The reason is that with vsini=17km/s, and 2% rotation amplitude signal, we expect an RV RMS of 300m/s at the Prot=3.5 day rotation period (vsini*rotation amplitude). This is probably larger than the expected planet signal (100m/s, 8 days).

4. THE PLANET

4.1. *Transit Fitting*

Simultaneous dip plus rotation period (GP) fit. Use celerite plus PyMC3/exoplanet. Mention FPP?

4.2. *Validation of TOI 837.01*

Exclude possibilities: "The transits are blended from a background, unassociated eclipsing binary system or transiting exoplanet: We take the same approach outlined in Vanderburg et al. (2019). In short, if the transits are a blend from the background system, the true radius ratio is constrained by the ratio of the ingress time (T12) to the..."

4.2.1. *Visual Binarity*

Figure 4 shows the scene. In the upper panels, the pixels used to measure the background level in the SPOC lightcurve are indicated with 'X' hatching, and the pixels used in the final lightcurve aperture are shown with '/' hatching.

Stars brighter than $T = 16$, as queried from the Gaia DR2 source catalog, are shown with orange circles. The relevant stars for a blend analysis are as follows.

- TOI 837 = TIC 460205581 (T=9.9). The target star.
- Star A = TIC 847769574 (T=14.6). 2.3" west. Proper motions and parallax imply it is comoving

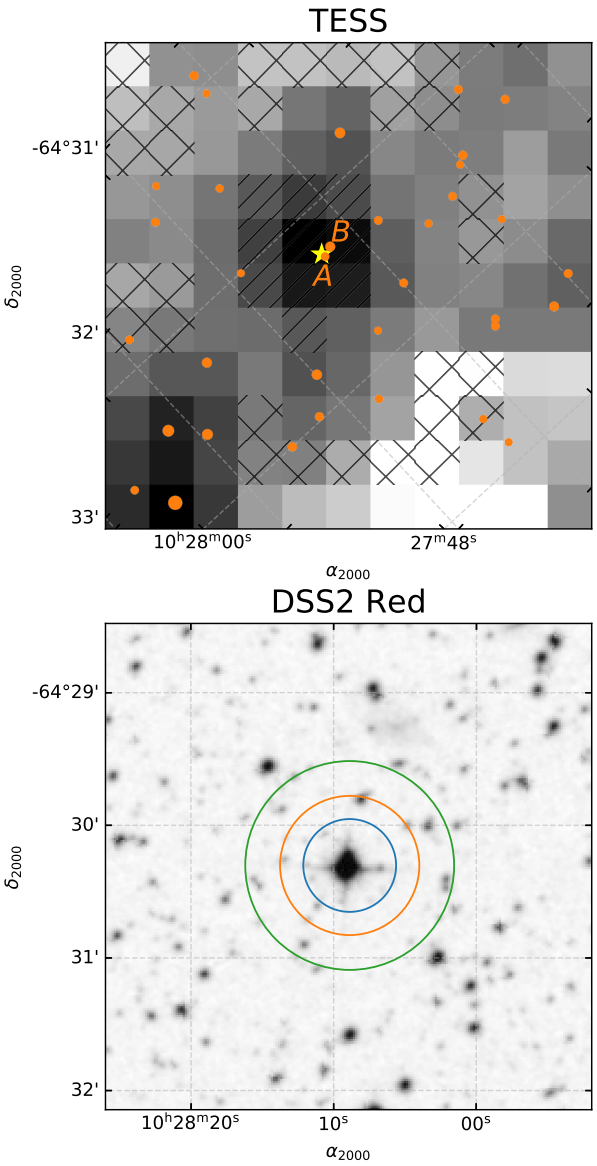

Figure 4. Scene used for blend analysis. *Top:* Mean TESS image of TOI 837 over Sector 10, with a logarithmic grayscale. The yellow star is the position of TOI 837. Orange circles are neighboring stars with $T < 16$, scaled such that brighter stars are larger. The X and / hatches show the apertures used to measure the background and target star flux, respectively. Dashed lines of constant declination and right ascension are shown. *Bottom:* Digitized Sky Survey *R*-band image of the same field, with a linear grayscale. The circles show apertures of radii 1, 1.5, and 2.25 pixels used in our blend analysis (Section **??**). Two stars of interest are "Star A" and "Star B", which were eventually excluded as being possible sources of the transits.

with TOI 837, though with a physical separation of 6.6 ± 0.1 pc, it may not be bound.

- Star B = TIC 460205587 (T=13.1). 5.4" north. This is a giant background star.

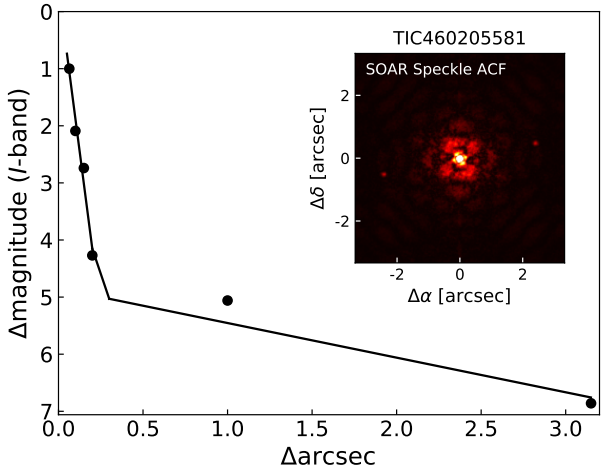

Figure 5. SOAR HRCam contrast limits derived from point-source injection-recovery experiments. Star A ($\Delta T = 4.7$, $\rho = 2.3$" west) is detected in the autocorrelation function, in addition to being a resolved Gaia source. It is co-moving with TOI 837, and its parallax and on-sky position imply that it is physically separated from TOI 837 by 6.6 ± 0.1 pc.

An additional source, TIC 847769581, is 4.9" from the target, but too faint (T=18.8) to be the source of the observed transit signal.

The Gaia DR2 data for Star A seems somewhat poorly behaved. While Star A has $G = 15.1$, and $Bp = 14.9$, no Rp magnitude is reported. Correspondingly, no RUWE value is available (CITE). The astrometric reduced χ^2 ($\chi^2/(N-5)$, for N the number of good astrometric observations) seems rather poor, at 8.6. We suspect that the photometric failure to produce an Rp magnitude, as well as the poor astrometric fit, are likely due to blending with TOI 837.

At the angular resolution of the TESS data, if either Star A or Star B were eclipsing binaries, they could be the sources of the transit signal. Coincidence stellar sources below the resolution limit of Gaia are also a concern (CITE). To rule out these possibilities, we took a number of approaches.

4.2.2. *High-resolution imaging*

We imaged the system using SOAR-HRCam. **Carl: please describe**. Figure 5. Ziegler et al. (2020)

4.2.3. *TESS analysis*

We examined the CDIPS FFI lightcurves of the target, which are available on MAST (Bouma et al. 2019). Three lightcurves are available, based on photometric apertures with a radius of 1, 1.5, or 2.5 pixels. In the raw difference-image light-curves, as well as the PCA-detrended light-curves, dips of depth ≈0.35% are visible, and their properties do not significantly vary with aperture size. Within ≈ 20", the dips are consistent with originating from the target star.

4.2.4. *Seeing-limited time-series photometry*

left off here Co-author P. Evans obtained a total transit that showed that, within 1.5", the transit comes from TOI 837.

We can be even more certain with a pixel-level analysis. This 2.1 arcsec neighbor is also a mid to late M dwarf, and bound given the Gaia parallax + proper motion. The transit duration is rather long for the signal to come from the M dwarf, rather than the G dwarf. I think the state of photometric followup could be improved (there is only one good total transit), but I think over this month and next we can pull another few partials.

A total eclipse of Ziegler's faint companion would produce a 1.4% dip. A 30% eclipse, more plausible for a NEB scenario, would produce dips at exactly the right depth (0.4%).

4.2.5. *Summary*

Possible false-positive scenarios are as follows.

- *Neighboring blends*.
- *Hierarchical blends*. Limited by i) FEROS + Veloce RVs, and ii) the star being nicely on the cluster HR diagram. Any extra hidden close-in binary stars would need to be very low-mass M dwarfs, and then the transit duration again helps.
- *Background blends*. Archival imaging (POSS) available in the south?

4.3. *Additional Companions*

None of the extra dips in the PDCSAP light-curve (e.g., "up-down" spikes at BTJD 1572 and 1601) seem likely to be planetary We checked that i) they were not present in the SAPFLUX light-curves, and ii) that they were not present in the CDIPS light-curves (either raw, or PCA-detrended).

To make this quantitative, we did injection-recovery.

5. DISCUSSION

In context,...

6. CONCLUSIONS

The authors thank... We also thank the Heising-Simons Foundation for their generous support of this work. The Digitized Sky Survey was produced at the Space Telescope Science Institute under U.S. Government grant NAG W-2166. Figure 4 is based on photographic data obtained using the Oschin Schmidt Telescope on Palomar Mountain.

Software: `astrobase` (Bhatti et al. 2018), `astropy` (Astropy Collaboration et al. 2018), `astroquery` (Ginsburg et al. 2018), `cdips-pipeline` (Bhatti et al. 2019) `corner` (Foreman-Mackey 2016), `exoplanet` (Agol et al. 2019) `exoplanet` (Foreman-Mackey et al. 2020), and its dependencies (Agol et al. 2019; Kipping 2013; Luger et al. 2019; Theano Development Team 2016). `IPython` (Pérez & Granger 2007), `lightkurve` (Lightkurve Collaboration et al. 2018), `matplotlib` (Hunter 2007), `MESA` (Paxton et al. 2011, 2013, 2015) `numpy` (Walt et al. 2011), `pandas` (McKinney 2010), `pyGAM` (Servén et al. 2018), `PyMC3` (Salvatier et al. 2016), `scipy` (Jones et al. 2001). `tesscut` (Brasseur et al. 2019), `wotan` (Hippke et al. 2019).

Facilities: *Astrometry*: Gaia (Gaia Collaboration et al. 2016, 2018). *Imaging*: Second Generation Digitized Sky Survey, Keck:II (NIRC2; www2.keck.hawaii.edu/inst/nirc2). *Spectroscopy*: Keck:I (HIRES; Vogt et al. 1994). *Photometry*: TESS (Ricker et al. 2015).

Table 1. Model Comparison.

Description	N_s	N_ℓ	N_{data}	N_{param}	χ^2	χ^2_{red}	BIC	ΔBIC
Favored	2	2	2585	17	3230.2	1.258	3363.7	0.0
Weakly favored	3	3	2585	21	3203.4	1.249	3368.4	4.7
—	3	2	2585	19	3222.9	1.256	3372.2	8.4
Disfavored	2	3	2585	19	3244.9	1.265	3394.2	30.4
—	2	1	2585	15	3410.6	1.327	3528.5	164.7
—	3	1	2585	17	3396.4	1.323	3530.0	166.3
—	1	2	2585	15	4158.6	1.618	4276.4	912.7
—	1	3	2585	17	4147.4	1.615	4281.0	917.2
—	1	1	2585	13	4313.5	1.677	4415.6	1051.9

NOTE— N_s and N_ℓ are the number of harmonics at the short and long periods, respectively. N_{data} is the number of fitted flux measurements. N_{param} is the number of free parameters in the model. The Bayesian information criterion (BIC) and the difference from the maximum ΔBIC are also listed.

Table 2. Best-fit model priors and posteriors.

Param.	Prior	Mean	Std. Dev.	3%	97%
P_s	$\mathcal{N}(0.4485; 0.0010)$	0.4484592	0.0000448	0.4483738	0.4485432
$t_s^{(1)}$	$\mathcal{N}(0.438096; 0.0020)$	0.438964	0.0011541	0.4367218	0.4410819
$R_p/R_\star$	$\mathcal{N}(0.1100; 0.0110)$	0.11461	0.00588	0.10407	0.12581
b	$\mathcal{U}(0; 1+R_p/R_\star)$	0.8103	0.0430	0.7279	0.8831
u_1	(2)	0.634	0.463	0.	1.492
u_2	(2)	0.033	0.404	-0.736	0.779
Mean	$\mathcal{U}(-0.01; 0.01)$	-0.000924	0.000195	-0.001275	-0.000539
ω_s	$2\pi/P_s$	14.01061	0.00140	14.00798	14.01327
$A_{s,0}$	$\mathcal{U}(-0.02; 0.02)$	0.009025	0.000383	0.008243	0.009695
$B_{s,0}$	$\mathcal{U}(-0.02; 0.02)$	0.009843	0.000383	0.009152	0.010563
$A_{s,1}$	$\mathcal{U}(-0.02; 0.02)$	0.001571	0.000337	0.000951	0.002223
$B_{s,1}$	$\mathcal{U}(-0.02; 0.02)$	-0.005324	0.000282	-0.005866	-0.004791
ϕ_ℓ	$\mathcal{U}(1.3721; 2.1575)$	1.75981	0.20755	1.40468	2.07790
ω_ℓ	$\mathcal{N}(12.6054; 0.1261)$	12.588617	0.000907	12.586906	12.590249
$A_{\ell,0}$	$\mathcal{U}(-0.06; 0.06)$	0.038302	0.004652	0.030051	0.044614
$B_{\ell,0}$	$\mathcal{U}(-0.06; 0.06)$	0.021721	0.008029	0.008567	0.034349
$A_{\ell,1}$	$\mathcal{U}(-0.02; 0.02)$	0.002271	0.000535	0.001288	0.003178
$B_{\ell,1}$	$\mathcal{U}(-0.02; 0.02)$	-0.00222	0.000539	-0.00309	-0.001201

(1) To convert mean TESS mid-transit time to BJD_{TDB}, add 2458468.2. (2) Quadratic limb-darkening prior from Kipping (2013), implemented by Foreman-Mackey et al. (2020).

REFERENCES

Agol, E., Luger, R., & Foreman-Mackey, D. 2019, arXiv e-prints, 1908.03222

Astropy Collaboration, Price-Whelan, A. M., Sipőcz, B. M., et al. 2018, AJ, 156, 123

Baratella, M., D'Orazi, V., Carraro, G., et al. 2020, Astronomy and Astrophysics, 634, A34

Bhatti, W., Bouma, L., & Yee, S. 2019, `cdips-pipeline v0.1.0`, https://doi.org/10.5281/zenodo.3370324

Bhatti, W., Bouma, L. G., & Wallace, J. 2018, `astrobase`, https://doi.org/10.5281/zenodo.1469822

Bossini, D., Vallenari, A., Bragaglia, A., et al. 2019, Astronomy and Astrophysics, 623, A108

Bouma, L. G., Hartman, J. D., Bhatti, W., Winn, J. N., & Bakos, G. Á. 2019, ApJS, 245, 13

Brasseur, C. E., Phillip, C., Fleming, S. W., Mullally, S. E., & White, R. L. 2019, Astrophysics Source Code Library, ascl:1905.007

Bravi, L., Zari, E., Sacco, G. G., et al. 2018, Astronomy and Astrophysics, 615, A37

Foreman-Mackey, D. 2016, The Journal of Open Source Software, 24

Foreman-Mackey, D., Czekala, I., Luger, R., et al. 2020, exoplanet-dev/exoplanet v0.2.6

Gaia Collaboration, Prusti, T., de Bruijne, J. H. J., et al. 2016, A&A, 595, A1

Gaia Collaboration, Brown, A. G. A., Vallenari, A., et al. 2018, A&A, 616, A1

Ginsburg, A., Sipocz, B., Madhura Parikh, et al. 2018, Astropy/Astroquery: V0.3.7 Release

Hippke, M., David, T. J., Mulders, G. D., & Heller, R. 2019, arXiv:1906.00966 [astro-ph], arXiv: 1906.00966

Hunter, J. D. 2007, Computing in Science & Engineering, 9, 90

Jones, E., Oliphant, T., Peterson, P., et al. 2001, Open source scientific tools for Python

Kipping, D. M. 2013, MNRAS, 435, 2152

Lightkurve Collaboration, Cardoso, J. V. d. M., Hedges, C., et al. 2018, Lightkurve: Kepler and TESS time series analysis in Python, Astrophysics Source Code Library, ascl:1812.013

Luger, R., Agol, E., Foreman-Mackey, D., et al. 2019, AJ, 157, 64

McKinney, W. 2010, in Proceedings of the 9th Python in Science Conference, ed. S. van der Walt & J. Millman, 51

Netopil, M., Paunzen, E., Heiter, U., & Soubiran, C. 2016, Astronomy and Astrophysics, 585, A150

Oh, S., Price-Whelan, A. M., Hogg, D. W., Morton, T. D., & Spergel, D. N. 2017, The Astronomical Journal, 153, 257

Paxton, B., Bildsten, L., Dotter, A., et al. 2011, ApJS, 192, 3

Paxton, B., Cantiello, M., Arras, P., et al. 2013, ApJS, 208, 4

Paxton, B., Marchant, P., Schwab, J., et al. 2015, ApJS, 220, 15

Pérez, F., & Granger, B. E. 2007, Computing in Science and Engineering, 9, 21

Ricker, G. R., Winn, J. N., Vanderspek, R., et al. 2015, Journal of Astronomical Telescopes, Instruments, and Systems, 1, 014003

Salvatier, J., Wieckiâ, T. V., & Fonnesbeck, C. 2016, PyMC3: Python probabilistic programming framework

Servén, D., Brummitt, C., & Abedi, H. 2018, dswah/pyGAM: v0.8.0

Theano Development Team. 2016, arXiv e-prints, abs/1605.02688

Vogt, S. S., Allen, S. L., Bigelow, B. C., et al. 1994, SPIE Conference Series, ed. D. L. Crawford & E. R. Craine, Vol. 2198

Walt, S. v. d., Colbert, S. C., & Varoquaux, G. 2011, Computing in Science & Engineering, 13, 22

Ziegler, C., Tokovinin, A., Briceño, C., et al. 2020, AJ, 159, 19